Bioorganic & Medicinal Chemistry 19 (2011) 2842–2849

Contents lists available at ScienceDirect

Bioorganic & Medicinal Chemistry

journal homepage: www.elsevier.com/locate/bmc

# Comparative CYP1A1 and CYP1B1 substrate and inhibitor profile of dietary flavonoids

Vasilis P. Androutsopoulos [a,*], Athanasios Papakyriakou [b], Dionisios Vourloumis [b], Demetrios A. Spandidos [a]

[a] Laboratory of Clinical Virology, University of Crete, Medical School, Voutes, 71003 Heraklion, Crete, Greece
[b] Laboratory of Chemical Biology of Natural Products and Designed Molecules, Institute of Physical Chemistry, NSCR 'Demokritos', 15310 Ag. Paraskevi, Athens, Greece

ARTICLE INFO

*Article history:*
Received 17 January 2011
Revised 10 March 2011
Accepted 18 March 2011
Available online 24 March 2011

*Keywords:*
P450
CYP1A1
CYP1B1
Cancer
Flavonoids
Chemoprevention
Homology modeling
Molecular docking

ABSTRACT

CYP1A1 and CYP1B1 are two extrahepatic enzymes that have been implicated in carcinogenesis and cancer progression. Selective inhibition of CYP1A1 and CYP1B1 by dietary constituents, notably the class of flavonoids, is a widely accepted paradigm that supports the concept of dietary chemoprevention. In parallel, recent studies have documented the ability of CYP1 enzymes to selectively metabolize dietary flavonoids to conversion products that inhibit cancer cell proliferation. In the present study we have examined the inhibition of CYP1A1 and CYP1B1-catalyzed EROD activity by 14 different flavonoids containing methoxy- and hydroxyl-group substitutions as well as the metabolism of the monomethoxylated CYP1-flavonoid inhibitor acacetin and the poly-methoxylated flavone eupatorin-5-methyl ether by recombinant CYP1A1 and CYP1B1. The most potent inhibitors of CYP1-EROD activity were the methoxylated flavones acacetin, diosmetin, eupatorin and the di-hydroxylated flavone chrysin, indicating that the 4′-$OCH_3$ group at the B ring and the 5,7-dihydroxy motif at the A ring play a prominent role in EROD inhibition. Potent inhibition of CYP1B1 EROD activity was also obtained for the poly-hydroxylated flavonols quercetin and myricetin. HPLC metabolism of acacetin by CYP1A1 and CYP1B1 revealed the formation of the structurally similar flavone apigenin by demethylation at the 4′-position of the B ring, whereas the flavone eupatorin-5-methyl ether was metabolized to an as yet unidentified metabolite assigned $E_5M1$. Eupatorin-5-methyl ether demonstrated a submicromolar $IC_{50}$ in the CYP1-expressing cancer cell line MDA-MB 468, while it was considerably inactive in the normal cell line MCF-10A. Homology modeling in conjunction with molecular docking calculations were employed in an effort to rationalize the activity of these flavonoids based on their CYP1-binding mode. Taken together the data suggest that dietary flavonoids exhibit three distinct modes of action with regard to cancer prevention, based on their hydroxyl and methoxy decoration: (1) inhibitors of CYP1 enzymatic activity, (2) CYP1 substrates and (3) substrates and inhibitors of CYP1 enzymes.



## 1. Introduction

Cytochrome P450s are heme containing enzymes that participate in the metabolism of various xenobiotics and endogenous substances. These enzymes catalyze a variety of chemical reactions such as O-dealkylation, N-dealkylation, O-hydroxylation and N-hydroxylation and thus play an important role primarily in phase I metabolism of xenobiotics facilitating their excretion, as well as in the activation of endogenous compounds (estradiol, testosterone, 11-deoxycortisol, arachidonic acid and vitamin D) to reactive conversion products that are involved in the regulation of physiological and cellular processes (homeostasis, endocrine control, inflammation and cellular proliferation).[1,2] The human cytochrome P450 family consists of three members CYP1A2, CYP1A1 and CYP1B1. CYP1A2 participates in phase I metabolism of drugs in the liver, whereas CYP1A1 and CYP1B1 are implicated in the activation of polycyclic aromatic hydrocarbons to carcinogenic intermediates in extrahepatic tissues.[1,3,4]

Due to the fundamental role of CYP1A1 and CYP1B1 in carcinogenesis, many studies have examined the interaction of the two enzymes with compounds that interfere with or inhibit the activation of carcinogens.[5–10] Flavonoids are polyphenolic molecules consisting of three rings (A, B and C) with documented substantial chemopreventive activity via the inhibition of CYP1-catalyzed carcinogenic product formation, DNA adduct production and tumor development in in vitro and in vivo models.[8–12] As a consequence, numerous studies have investigated the in vitro inhibitory activity of several classes of naturally occurring flavonoids, in order to provide insight for the potential of dietary chemoprevention.[5,13] Some monomethoxylated flavonoids such as the flavonoid chrysoeriol inhibit recombinant CYP1B1 EROD activity as well as oestradiol 4-hydroxylation and dihydroxy-9,10-epoxy-7,8,9,10-tetrahydrobenzo[*a*]pyrene-$N^2$-deoxyguanosine adducts in MCF-7 cells.[14,15]

* Corresponding author. Tel.: +30 2810 394870; fax: +30 2810 542098.
*E-mail address:* vandrou@med.uoc.gr (V.P. Androutsopoulos).

0968-0896/$ - see front matter © 2011 Elsevier Ltd. All rights reserved.
doi:10.1016/j.bmc.2011.03.042

**Table 1**
$K_i$ values of flavonoids for CYP1A1 and CYP1B1 derived from $IC_{50}$ and $K_m$ values for each flavonoids and enzyme, respectively. Results are expressed as mean ± SD of at least $n = 3$ determinations

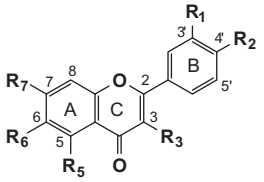


| Compound | $R_1$ | $R_2$ | $R_3$ | $R_5$ | $R_6$ | $R_7$ | $K_i$ (μM) | |
|---|---|---|---|---|---|---|---|---|
| | | | | | | | CYP1A1 | CYP1B1 |
| Chrysin | H | H | H | OH | H | OH | 0.042 ± 0.006 | 0.016 ± 0.004 |
| Apigenin | H | OH | H | OH | H | OH | 0.39 ± 0.01 | 0.064 ± 0.010 |
| Luteolin | OH | OH | H | OH | H | OH | 0.89 ± 0.06 | 0.056 ± 0.011 |
| Baicalein | H | H | H | OH | OH | OH | 1.22 ± 0.90 | 0.26 ± 0.01 |
| Scutellarein | H | OH | H | OH | OH | OH | 1.64 ± 0.21 | 0.22 ± 0.007 |
| Acacetin | H | $OCH_3$ | H | OH | H | OH | 0.045 ± 0.02 | 0.007 ± 0.003 |
| Diosmetin | OH | $OCH_3$ | H | OH | H | OH | 0.089 ± 0.07 | 0.016 ± 0.089 |
| Eupatorin | OH | $OCH_3$ | H | OH | $OCH_3$ | $OCH_3$ | 0.21 ± 0.006 | 0.035 ± 0.004 |
| Eupatorin-5-OMe | OH | $OCH_3$ | H | $OCH_3$ | $OCH_3$ | $OCH_3$ | 0.63 ± 0.03 | 0.67 ± 0.04 |
| Genkwanin | H | OH | H | OH | H | $OCH_3$ | >2.34 | >2.34 |
| Cirsiliol | OH | OH | H | OH | $OCH_3$ | $OCH_3$ | >0.8 | >0.8 |
| Kaempherol | H | H | OH | OH | H | OH | 0.75 ± 0.13 | 0.043 ± 0.007 |
| Quercetin | OH | OH | OH | OH | H | OH | 0.66 ± 0.01 | 0.023 ± 0.01 |
| Myricetin* | OH | OH | OH | OH | H | OH | 0.37 ± 0.01 | 0.027 ± 0.007 |

* Ring B(5′-OH).

The results suggested that selective inhibition occurred in the cells.[14,15] Flavonoids with multiple hydroxyl groups have been documented as effective CYP1 inhibitors, whereas little is known regarding the inhibitory activities of poly-methoxylated flavonoids on CYP1 enzymes. Recent studies suggest that CYP1A1 and CYP1B1 enzymes show substrate specificity for flavonoids with multiple methoxy-groups.[16] The latter enzymes promote demethylation reactions at various positions of the polyphenolic moiety, notably the 4′-position of the B ring, which gives rise to metabolites with increased pharmacological and antiproliferative activity.[17–19] It has been postulated that dietary flavonoids exhibit cancer therapeutic effects, due to intracellular CYP1-mediated metabolism to conversion products that inhibit growth of cancerous cells.[16–20] Thus the duality of flavonoids in cancer therapy and prevention is determined by both, their substrate and inhibitor propensities towards CYP1A1 and CYP1B1 enzymes.[16]

Inhibition of 7-ethoxyresorufin-*O*-deethylase activity (EROD) is a well documented assay used predominantly to test the inhibitory potencies of dietary flavonoids. In addition to EROD, several studies have employed molecular modeling analyzes to examine the flavonoid-inhibitor binding or substrate orientation of prototype ligands within the CYP1 enzyme active site.[21,22] In the present study we have examined the EROD-inhibitory activities of a range of hydroxylated and methoxylated flavonoids (Table 1) towards CYP1A1 and CYP1B1, as well as the metabolism of the monomethoxylated flavone acacetin and the poly-methoxylated flavone eupatorin-5-methyl ether by both enzymes. A homology model was further constructed using the CYP1A2 crystal structure as a template, and the binding mode of selected flavonoids to the heme group was investigated. Based on our previous findings, our aim was to provide a comparison between substrate–inhibitor binding affinities of hydroxylated and methoxylated flavonoids that could be supported by experimental and molecular docking results.

## 2. Results and discussion

### 2.1. Inhibition

The inhibitory potencies of dietary flavonoids towards CYP1A1 and CYP1B1 enzymes have been investigated by various in vitro models. EROD assay is one of the most popular screening tools for identifying this type of activity. Notably, flavonoids inhibit the de-alkylation of 7-ethoxyresorufin to resorufin and not the overall activity of CYP1B1 or CYP1A1.[9,13,23] Although the CYP1A1/CYP1B1-EROD catalyzed inhibition is evident for many poly-hydroxylated and some monomethoxylated flavonoids, little is known regarding the EROD-inhibitory activities of poly-methoxylated flavonoids. In light of our recent discoveries on the CYP1A1/CYP1B1-catalyzed metabolism of dietary flavonoids, we evaluated the EROD-inhibitory activities of flavonoids with different hydroxyl- and methoxy-substitutions. Since many of the flavonoids have been documented to be substrates for CYP1 enzymes, we expected at least a partial inhibition of CYP1B1 and CYP1A1–EROD activity, due to substrate-binding competition to the heme group.

Initial experiments involved 7-ER-*O*-deethylase kinetics assessment by measuring the rate of resorufin production over time. At a concentration range of 0.01–5 μM the deethylation of 7-ER by CYP1A1 or CYP1B1 followed Michaelis–Menten kinetics (Fig. 1A). At higher concentrations (>5 μM) the enzyme activity decreased indicating substrate inhibition (data not shown). Apparent Kinetic parameters were estimated using GraphPad Prism and were 0.52 μM ($K_m$) and 24.7 pmol/min/pmol of enzyme ($V_{max}$) for CYP1A1 and 0.17 μM ($K_m$) and 9.07 pmol/min/pmol of enzyme ($V_{max}$) for CYP1B1.

Percentage of EROD activity was plotted against flavonoid concentration and the $IC_{50}$ estimated by sigmoidal dose–response curves (Fig. 1B and C). $K_i$s were calculated using $IC_{50}$ values for each flavonoid and $K_m$ parameters for CYP1A1 and CYP1B1 (Table 1). The most potent inhibitors of CYP1B1–EROD activity were the flavones acacetin, chrysin and diosmetin with $K_i$s of 0.007, 0.016 and 0.016 μM, respectively (Table 1). Compounds with similar magnitude of potency with respect to CYP1B1–EROD inhibition were the flavonols quercetin, myricetin and kaempferol, whereas the poly-methoxylated flavone eupatorin exhibited a $K_i$ of 0.035 μM. The hydroxylated flavones apigenin and luteolin showed slightly higher CYP1B1-inhibition compared to the previously mentioned compounds, while baicalein, scutellarein and eupatorin-5-methyl ether were moderate inhibitors of CYP1B1–EROD activity. The flavones genkwanin and cirsiliol were the weakest inhibitors of all compounds tested.

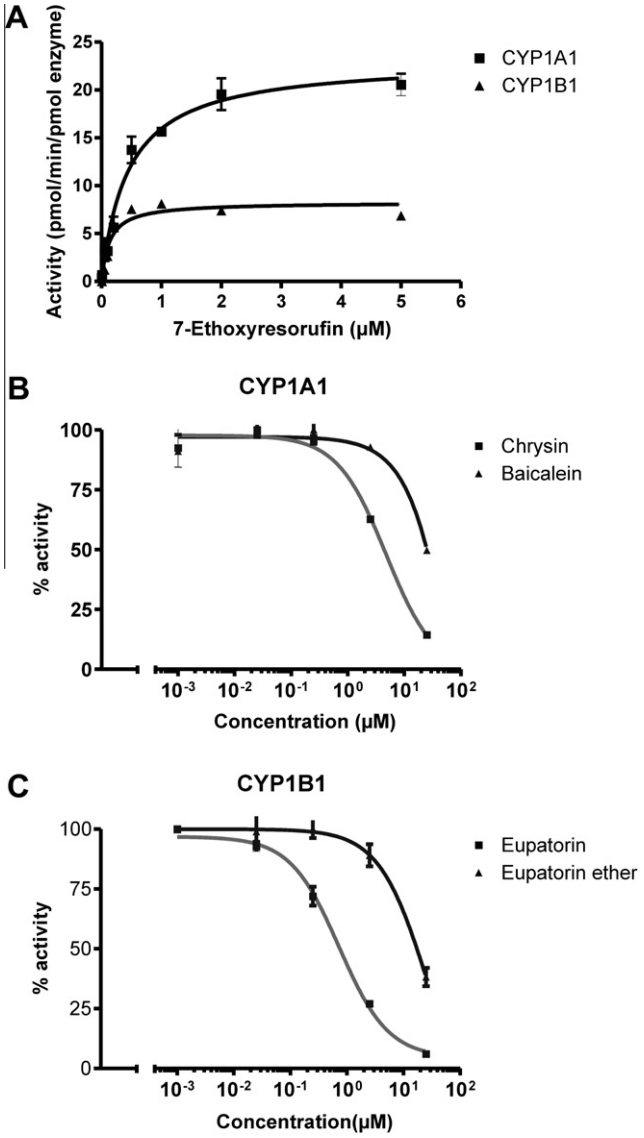


**Figure 1.** Inhibition of 7-ethoxyresorufin deethylase activity by dietary flavonoids. (A) Michaelis–Menten kinetics of 7-ethoxyresorufin deethylation. 7-Ethoxy resorufin was incubated at a concentration range of 0.005–5 μM with CYP1A1 or CYP1B1 in the presence of NADPH (0.5 mM), $H_2PO_4$ (20 mM) and $MgCl_2$ (5 mM) at 37 °C for 15 min. Fluoresence of resorufin production was measured at excitation 530 nm and emission 590 nm. The amount of resorufin produced was normalized against time and enzyme concentration and apparent $V_{max}$ and $K_m$ parameters were estimated using GraphPad Prism software. (B) Dose–response curves of flavonoid-mediated inhibition of CYP1A1 EROD activity and (C) of CYP1B1–EROD activity. Inhibition EROD experiments containing flavonoids were performed as described in Section 4. Error bars represent mean ± SD for at least four independent experiments.

CYP1A1–EROD activity was affected to a lesser extent by dietary flavonoids than CYP1B1. The most potent CYP1A1-catalyzed EROD inhibitor was acacetin and chrysin with a $K_i$ of 0.045 and 0.042 μM, respectively, followed by diosmetin ($K_i$ = 0.089 μM) (Table 1). The poly-methoxylated flavone eupatorin was also a strong CYP1A1-catalyzed EROD inhibitor ($K_i$ = 0.21 μM) followed by the hydroxylated flavone apigenin and the hydroxylated flavonol myricetin. Eupatorin-5-methyl ether, kaempferol, quercetin and luteolin demonstrated intermediate efficacies with respect to CYP1A1-catalyzed EROD inhibition, with $K_i$s varying between 0.63 and 0.89 μM. The weakest inhibitors were baicalein, scutellarein, genkwanin and cirsiliol.

## 2.2. Metabolism

Cytochrome P450 CYP1-mediated metabolism of dietary flavones has been documented in our previous studies.[17–20,24] We have identified the 4′-$OCH_3$ methoxy group present at the B ring of the flavonoid structure as a key determinant of CYP1A1/CYP1B1-catalyzed substrate turnover.[17–19] In addition poly-hydroxyl flavones (e.g., scutellarein) are less efficient substrates with regard to CYP1A1 rate of metabolism, as opposed to polymethoxy-flavones (e.g., sinensetin).[20] Our current study advances to provide further information regarding the metabolic turnover of the poly-methoxylated flavonoid eupatorin-5-methyl ether by CYP1A1 and CYP1B1. Eupatorin-5-methyl ether (Table 1) is a component of the plant *Orthosiphon stamineus* that also contains the flavones eupatorin and sinensetin, and has been shown to possess anti-inflammatory activity.[25] Herein we demonstrate that eupatorin-5-methyl ether is metabolized by recombinant CYP1A1 or CYP1B1 enzymes over a 20 min period (Fig. 2A). CYP1B1 was a very weak metabolizer of eupatorin-5-methyl ether compared to CYP1A1 (Fig. 2B). HPLC analysis indicated the presence of an unidentified metabolite, assigned $E_5M1$, eluting at approximately 8.9 min following incubation of the compound with CYP1 enzymes. In an effort to identify $E_5M1$ we performed co-elution studies with eupatorin, which possesses a hydroxyl group at position 5 of the A ring. A CYP1A1-eupatorin-5-methyl ether incubate was spiked with a eupatorin standard. The analysis showed the eupatorin does not co-elute with $E_5M1$ (Fig. 2A). We further tested the ability of eupatorin-5-methyl ether to inhibit proliferation of breast cancer cells in the CYP1 expressing cell line MDA-MB 468 by the MTT assay. Eupatorin-5-methyl ether possessed strong antiproliferative activity in MDA-MB 468 cells, whereas it was considerably inactive in the non-CYP1 expressing cell line MCF-10A (Fig. 2C).

In addition to eupatorin-5-methyl ether, the metabolism of the monomethoxylated flavone acacetin by CYP1A1 and CYP1B1 was investigated. Acacetin is a flavone present in citrus fruits that has demonstrated strong inhibition of CYP1-catalyzed EROD activity.[13] Acacetin was metabolized weakly by CYP1A1 to two major and two minor metabolites (Fig. 3A). CYP1B1 revealed an even slower rate of metabolism (Fig. 3B). Co-elution studies for metabolite identification proved that acacetin undergoes demethylation to the 4′-position to apigenin and further hydroxylation to the 6-position to scutellarein and to the 3′-position to luteolin (Fig. 3A, Table 1). An unidentified metabolite assigned $AM_1$ with retention time of 11.3 min was also noted. Apigenin was produced by CYP1A1 at a greater rate compared to CYP1B1 over a 20 min period (Fig. 3C). Based on the identification pattern and the conversion rate of each metabolic product (Fig. 3A) it is seemingly obvious that luteolin and scutellarein arise mainly by secondary metabolism of apigenin by CYP1 enzymes. This is because formation of these two flavones by acacetin would require an additional intermediate metabolite (possibly $AM_1$) arising by hydroxylation at either the 6-position of the A ring or the 3′-position of the B ring of acacetin and further demethylation to the 4′-position to yield either luteolin or scutellarein. Given the conversion rate of luteolin formation (Fig. 3A) this step is unlikely to occur through metabolism to $AM_1$. As a result metabolism of acacetin by CYP1A1 and CYP1B1 yields mainly apigenin and the metabolite $AM_1$ (Fig. 3A).

## 2.3. Ligand binding

### 2.3.1. EROD and HPLC studies conclusions

Based on the results reported herein and our previous studies it is conceivable that a strong EROD inhibition or an HPLC metabolic profile alone are not sufficient for determining the inhibitor/substrate mode of action of a certain flavonoid towards CYP1A1. Table 2 summarizes the CYP1A1/CYP1B1-catalyzed rate of metabolism as

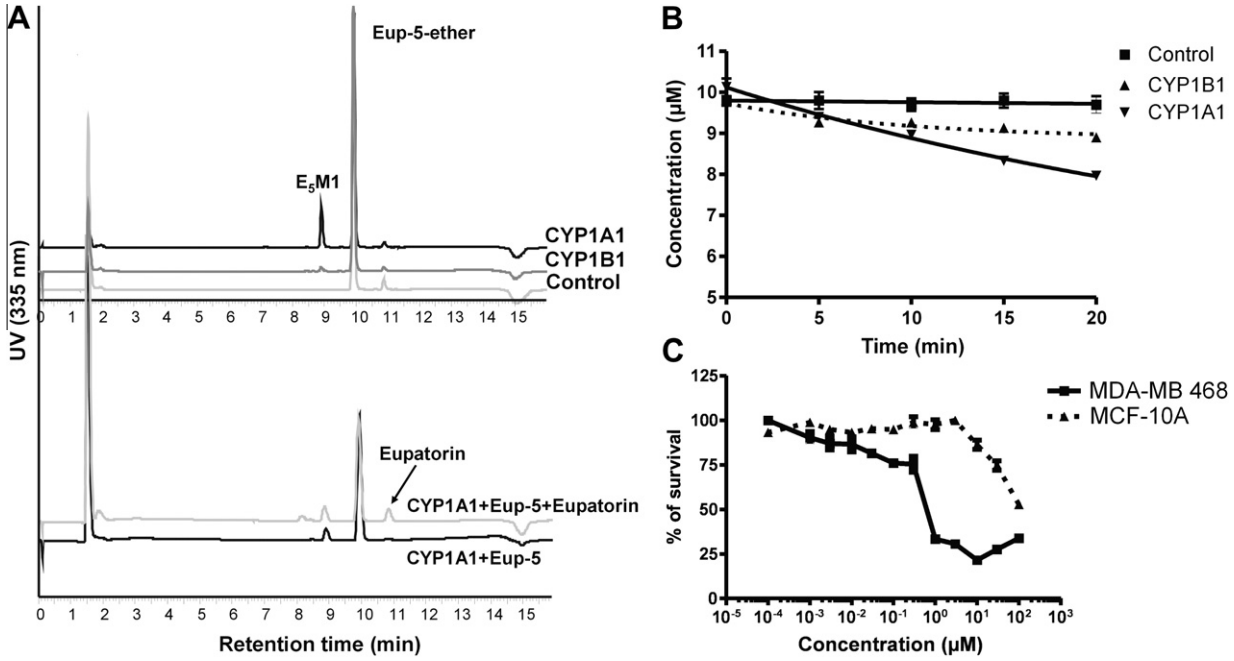


**Figure 2.** The metabolism of eupatorin-5-methyl ether by CYP1A1 and CYP1B1 and its cytotoxicity in MDA-MB-468 and MCF-10A cells. Eupatorin-5-methyl ether (10 μM) was incubated with recombinant CYP1A1 and CYP1B1 for 20 min as described in Section 4. (A) Metabolic profile and co-elution studies of a 20 min incubate with eupatorin A 20 min incubate was spiked with authentic standard solution (1 μM) containing eupatorin. (B) Rate of metabolism of eupatorin-5-methyl ether by CYP1A1 and CYP1B1 over 20 min. (C) MTT assay of eupatorin-5-methyl ether in MDA-MB-468 and MCF-10A cells.

well as the cytotoxicity $IC_{50}$ values in MDA-MB-468 and MCF-10A cell lines of various dietary flavonoids, as demonstrated by this report and our previous studies. Rate of metabolism is presented as the percentage of parent compound remaining at the 20 min incubation by recombinant CYP1A1 (20 min incubate) and is estimated by the fraction: flavonoid concentration of CYP1A1 incubate/flavonoid concentration of control incubate, as described in detail in Section 4. For example, diosmetin and eupatorin show strong EROD inhibition activities, however the CYP1A1-catalyzed metabolic rate is considerably high (51.3% and 47.8% conversion, respectively, Table 2). This suggests that these two compounds are substrates for CYP1A1 and thus the potency obtained in EROD activity assay originates from substrate competition binding with 7-ethoxy resorufin. Consistent with this conclusion is the finding that both of these flavones are metabolized and activated in CYP1A1/CYP1B1 expressing cell lines. On the other hand acacetin and chrysin show a very poor metabolic profile with respect to CYP1A1-catalyzed rate of metabolism (Table 2 and 15.9% and 15.9%, respectively). In addition the latter compounds exhibited potent inhibition of EROD activity. This suggests that they act as potent inhibitors of CYP1A1 rather than substrates. A third category of compounds includes those that exhibit CYP1A1 substrate and inhibitor propensities. Examples of this category are compounds such as the di-methoxylated flavone cirsiliol and the tetra-hydroxylated scutellarein, for which a weak inhibition of CYP1A1-catalyzed EROD activity is obtained, as well as an intermediate rate of metabolism (16.7% and 12.6% conversion, respectively, Table 2) and baicalein that presents no substrate metabolism with weak EROD inhibitory profile for CYP1A1.

CYP1B1 exhibits a dissimilar pattern of flavonoid metabolic turnover and flavonoid–EROD inhibition compared to CYP1A1. CYP1B1 was affected to a greater extent by flavonoid-mediated inhibition of EROD activity, as flavonoid $K_i$s for CYP1B1 were lower than those obtained for CYP1A1 (with the exception of eupatorin-5-methyl ether). In addition CYP1B1 is a weaker metabolizer of flavonoids with respect to the amount of metabolic product formed, as opposed to CYP1A1. These initial observations suggest that the differences noted for CYP1A1 and CYP1B1 in inhibition of EROD-catalyzed activities by flavonoids, as well as the dissimilarities in flavonoid metabolic turnover may be attributed to the orientation of the molecules to the heme group and the catalytic binding domain.

### 2.3.2. Molecular modeling

Homology models of CYP1A1 and CYP1B1 based on the crystallographic structure of CYP1A2 have been used recently to elucidate estradiol hydroxylation.[26] Consistent with the results presented earlier by Lewis et al.,[27–29] relatively small changes between the active site regions have been employed in the rationalization of CYP1 enzyme preferences for particular substrate types. Flavonoid-binding to the catalytic domain of CYP1A1 and CYP1B1 has been investigated by a paucity of studies. Iori et al.[22] examined the binding of flavonoids to the CYP1A1 and CYP1A2 active site using molecular modeling. Flavonoids carrying several hydroxyl groups, such as quercetin and myricetin were predicted to reside in close proximity to the heme site, leaving the catalytic site unperturbed. In a recent study,[23] it was demonstrated that Ser122 of CYP1A1 and Ala133 of CYP1B1 play an important role in the selectivity of methoxy-flavonoids for inhibition of CYP1A1/CYP1B1-catalyzed EROD activity.

Molecular modeling can support the inhibitory and substrate profile of the flavonoids studied, as well as earlier observations on the role of specific residues of CYP1A1, such as Ser122, Phe258 and Leu312. Our docking results indicate a good correlation between the predicted affinities of the flavonoids studied for CYP1A1 and CYP1B1 (Tables S1 and S2, Supplementary data). In particular, the average difference between the calculated and the experimental binding free energy for CYP1A1–flavonoids is only 0.8 kcal $mol^{-1}$, whereas for CYP1B1–flavonoids is 2.2 kcal $mol^{-1}$. This difference reflects the fact that the homology model of CYP1A1 is based on the high sequence identity structure of CYP1A2 (Fig. S1, Supplementary data), in contrast to the lower sequence

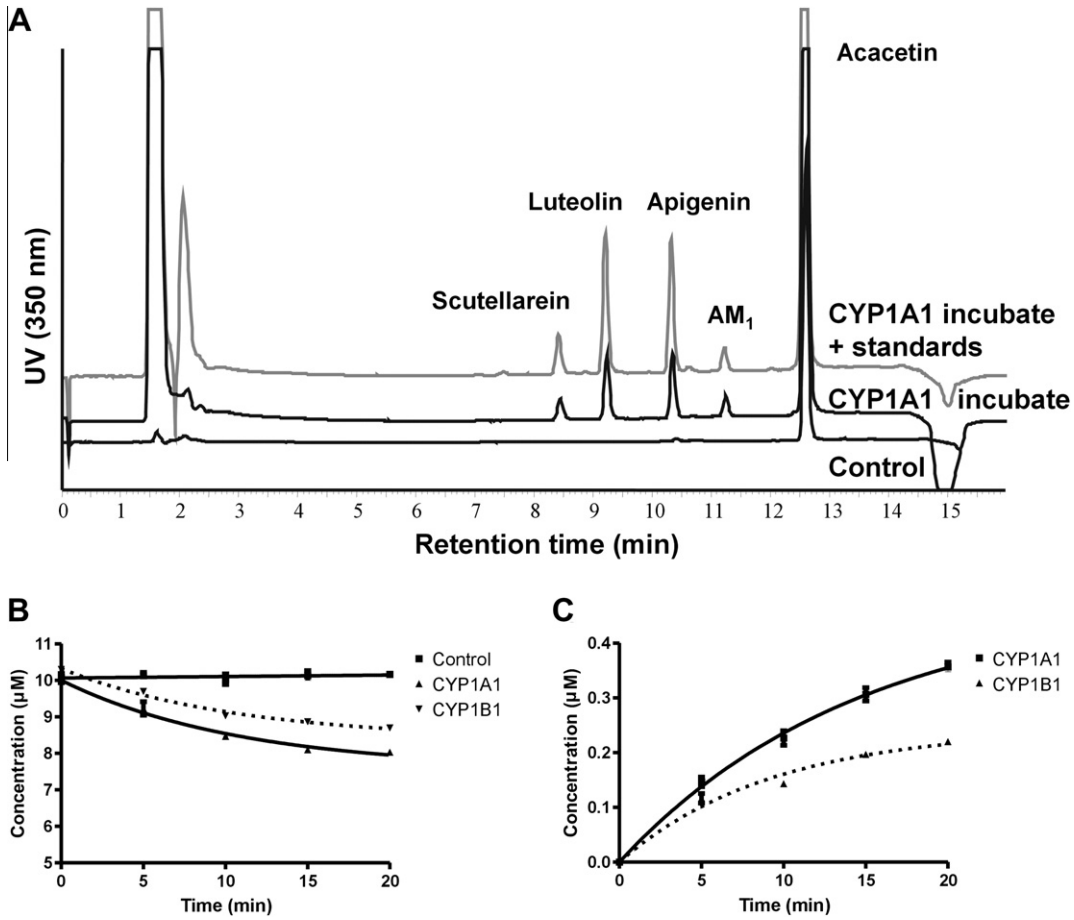


**Figure 3.** The metabolism of acacetin by CYP1A1 and CYP1B1. Acacetin (10 μM) was incubated with recombinant CYP1A1 and CYP1B1 for 20 min as described in Section 4. (A) Metabolic profile and identification of metabolites formed after a 20-min incubate. Incubates were spiked with authentic standard solutions (1 μM) containing apigenin, scutellarein and luteolin. (B) Rate of metabolism of acacetin by CYP1A1 and CYP1B1. (C) Formation of apigenin by CYP1A1 and CYP1B1 catalyzed metabolism over a 20-min period.

identity of CYP1B1 for CYP1A2 and CYP2C9 (Fig. S2, Supplementary data). Therefore, our observations are based mainly on the residue-specific interaction within the binding cavity of CYP1A1.

The simulated binding orientation of the flavonoids studied (Fig. 4) is in accordance with previous reports and a recent study by Takemura et al.[23] Diosmetin and eupatorin are predicted to bind CYP1A1 with ring-B over the prosthetic group so that 4′-methoxy group is at ~4.5 Å from the heme iron (Fig. 4A and B, respectively). Diosmetin is accommodated within the active site via extensive non-polar contacts and hydrogen bonding interactions, including that between O1 of ring C and the side chain of Ser122, which is replaced by Ala133 in CYP1B1. This difference may account for the selective CYP1A1 4-*O*-demethylation of diosmetin to luteolin.[18,19] Similarly, the conversion of eupatorin to cirsiliol was catalyzed by CYP1A1 with a comparable rate (~48% vs 51% of diosmetin, Table 2). Our modeling results indicate that the 4′-methoxy group approaches the catalytic heme so that the 3′-OH forms a hydrogen bond with the backbone of Leu496. At this orientation eupatorin is not predicted to interact with Ser122 of CYP1A1, but instead interacts with Asn221 side chain amide that forms a hydrogen bond with O4 of ring C (Fig. 4B). Hydrophobic interactions between the methoxylated ring B and Phe258, Phe224, Leu312 and Ile115 provide additional stabilization of the CYP1A1–eupatorin complex.

The less-substituted chrysin and acacetin (Fig. 4C and D) were also predicted to bind CYP1A1 in the same orientation with ring B over the iron–heme group. In this context, chrysin was predicted to be stabilized via a hydrogen bond with Ser122 hydroxylate group, whereas acacetin via a hydrogen bond with Asn221, as in the cases of diosmetin and eupatorin, respectively. However, their poor metabolic rate (Table 2) might be a consequence of the lower number of interactions, either hydrophobic or polar, within the active site of CYP1A1.

**Table 2**
CYP1A1 rate of metabolism of dietary flavonoids and activation factor in the CYP1 expressing cell line MDA-MB468. Rate of metabolism was expressed as percentage of parent-flavonoid-compound remaining at 20 min incubation with CYP1A1 microsomes and calculated by the fraction = concentration of CYP1A1 microsome flavonoid incubate/concentration of control microsome flavonoid incubate. Activation factor is derived by dividing the $IC_{50}$ of each compound in the normal MCF-10A cell line that does not express CYP1A1 with the $IC_{50}$ in the cancer cell line MDA-MB 468

| Compound | CYP1A1 rate of metabolism (%) | Activation factor MCF10A/MDA468 | References |
|---|---|---|---|
| Sinensetin | 68.9 | 325 | 20 |
| Diosmetin | 51.3 | 20 | 18,19 |
| Eupatorin | 47.8 | 100 | 17 |
| Genkwanin | 34.0 | 47 | 20 |
| Eupatorin-5-OMe | 20.4 | 100 | This study |
| Cirsiliol | 16.7 | 8 | 17 |
| Acacetin | 15.9 | — | This study,17 |
| Chrysin | 15.9 | 1.1 | 20 |
| Scutellarein | 12.6 | 3.3 | 20 |
| Baicalein | — | 1.7 | 20 |

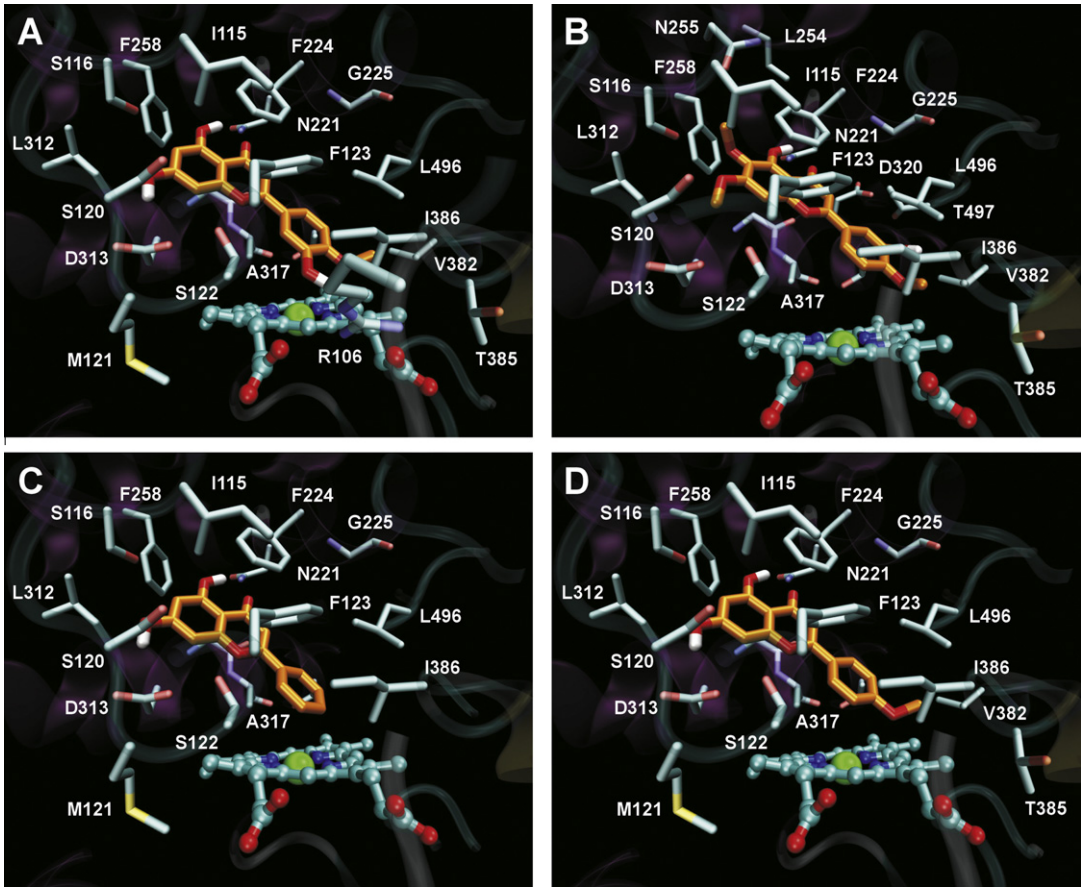


**Figure 4.** Human CYP1A1 active site models in complex with (A) diosmetin, (B) eupatorin, (C) chrysin and (D) acacetin. The four substrates (orange sticks) and the amino acid residues that constitute the active site cavity (cyan sticks), including the heme group, are shown. Nitrogen, oxygen and iron atoms are colored blue, red and green, respectively.

### 2.4. Biological activity

The relative substrate or inhibitor propensities of dietary flavonoids will determine their mode of action with regard to cancer prevention. Based on previous studies from our group and others and the results presented herein, it is evident that dietary flavonoids can act as CYP1A1/CYP1B1 substrates or inhibitors or both. Flavonoids with multiple hydroxyl groups are generally thought to be better inhibitors of CYP1A1 and CYP1B1 enzymes than substrates, and as a result may present chemopreventative properties by inhibiting the production of carcinogenic metabolites (benzo[a]pyrene 7,8-diol epoxide, 2,4-hydroxy-oestradiol).[30,3] In marked contrast, flavonoids that contain multiple methoxy groups have been shown to possess higher metabolic turnover by CYP1A1 and CYP1B1.[17,20] It is generally believed that high CYP1A1/CYP1B1 metabolic turnover of methoxylated flavonoids attributes to enhanced antiproliferative activity, even though such an outcome would depend on several factors, such as site of hydroxylation/demethylation, rate of metabolism, number of metabolites, predominant metabolic product conversion and biological activity of each metabolite. Despite this fact several CYP1A1/CYP1B1-catalyzed flavonoid metabolites have been shown to inhibit cancer cell cycle progression, as documented by our previous reports.[17–20] Luteolin, the main conversion product of diosmetin CYP1-mediated metabolism, is an EGFR inhibitor, apigenin (Fig. 4) is the metabolite of CYP1-catalyzed conversion of genkwanin or acacetin, a MAPK kinase inhibitor and cirsiliol is the metabolite of eupatorin, that induces G2/M arrest in cancerous cells.[17,31,32] A combination of the two modes of action is also possible, as a dietary flavonoid may present CYP1-inhibitory and CYP1-metabolic turnover activities, whereas the arising metabolite may equally act as a CYP1 inhibitor or a CYP1 substrate.

## 3. Conclusions

In summary, the current study examined the CYP1A1/CYP1B1–EROD catalyzed inhibitory activities of a range of methoxylated and hydroxylated flavonoids and the CYP1A1/CYP1B1 metabolism of the monomethoxylated flavone acacetin and the poly-methoxylated flavone eupatorin-5-methyl ether. The data suggest that compounds that show high rate of metabolism by CYP1A1 may appear as strong inhibitors of CYP1A1-catalyzed EROD activity, whereas compounds that show intermediate potencies of CYP1A1-catalyzed EROD activity may act simultaneously as substrates and inhibitors of CYP1A1. Molecular docking reveals favorable energies for poly-methoxylated flavonoids with respect to binding orientations to the heme group, as opposed to poly-hydroxylated flavonoids. Inhibition of CYP1B1-catalyzed EROD activity is affected to a greater extent by dietary flavonoids compared to CYP1A1, while with regard to flavonoid rate of metabolism CYP1B1 shows much slower rate compared to CYP1A1. Our findings contribute interesting insight to the CYP1A1/CYP1B1 substrate–inhibitor–flavonoid modes of action and as a result to their corresponding chemopreventative activity.

## 4. Materials and methods

### 4.1. Materials

Apigenin (95% pure), luteolin (98% pure), quercetin (98% pure), myricetin (85% pure), kaempferol (90% pure), chrysin (96% pure) and baicalein (98% pure) were obtained from Sigma (Poole UK), diosmetin, scutellarein and sinensetin (99% pure) from Indofine (Hillsborough, NJ, USA) and eupatorin, eupatorin-5-methyl ether, cirsiliol and genkwanin (97% pure) from Lancaster (Heysham, UK). Stock solutions were prepared in dimethyl sulfoxide and stored at −20 °C. 7-Ethoxy resorufin was purchased from Sigma (Poole UK), prepared as 1 mM stock solution in dimethylsulfoxide and kept at 4 °C. CYP1 supersomes were purchased from BD Biosciences (Cowley UK). Solvents for the HPLC analyzes were of HPLC grade and purchased from Fisher (Loughborough, UK).

### 4.2. EROD assays

7-Ethoxy resorufin (7ER) was incubated at a concentration range of 0.005–5 μM with CYP1A1 or CYP1B1 in the presence of NADPH (0.5 mM), $PO_4$ buffer (20 mM) and $MgCl_2$ (5 mM). The reaction was carried out in a shaking incubator at 37 °C for 15 min. The reaction was terminated by addition of equal volumes of ice-cold methanol. The samples were centrifuged at 13,000 rpm for 5 min and the supernatant removed. Fluoresence of resorufin production was measured at excitation 530 nm and emission 590 nm. Standard curves of resorufin were produced at a concentration range of 0.01–5 μM. The amount of resorufin produced was normalized against time and enzyme concentration. The data were fitted to Michaelis–Menten equation and apparent $V_{max}$ and $K_m$ parameters estimated using GraphPad Prism software.

Inhibition experiments containing flavonoids were performed as described above in the presence of each flavonoid at a concentration range of 0.0025–25 μM. The amount of resorufin formed was normalized against time and enzyme concentration and plotted versus inhibitor concentration. The $IC_{50}$ was determined as the concentration of the inhibitor responsible for 50% inhibition of EROD activity from a sigmoidal dose–response curve. $K_i$s were calculated using the formula $K_i = IC_{50}/(1 + [S]/K_m)$ for each inhibitor, where [S] is the concentration of 7-ER used in each assay and $K_m$ the Michaelis–Menten constant for the 7-*O*-deethylation of 7-ER by CYP1A1 or CYP1B1. Results are expressed as means ± SD for at least $n = 3$ determinations.

### 4.3. HPLC metabolism of acacetin and eupatorin-5-methyl ether

Eupatorin-5-methyl ether or acacetin (10 μM) were incubated with CYP1A1 or CYP1B1 in the presence of $PO_4$ (20 mM), $MgCl_2$ (5 mM) and NADPH (0.5 mM) for 20 min. Samples were taken in 5 min intervals and the reaction was terminated by addition of an equal volume of 1% acetic acid in methanol. The samples were centrifuged at 13,000 rpm for 5 min and the supernatant transferred to glass vials and analyzed by HPLC as described in previous methodologies.[17] For co-elution studies a 20 min CYP1A1 or CYP1B1 incubate was spiked with 0.5–1 μM of a flavonoid standard and the resulting sample analyzed by HPLC. UV detection used for eupatorin-5-methyl ether was at 335 nm and for acacetin and metabolites at 350 nm. Control incubations were performed with insect cell microsomes free of human cytochromes purchased commercially by GENTEST (BD Biosciences, UK). Rate of metabolism was expressed as percentage of parent-flavonoid-compound remaining at 20 min incubation with CYP1A1 microsomes and calculated by the fraction Rate = Concentration of CYP1A1 microsome flavonoid incubate/concentration of control microsome flavonoid incubate.

### 4.4. Cell culture and MTT assay

Cell culture and MTT methodologies were performed as described in previous studies.[17]

### 4.5. Computational methods

#### 4.5.1. Homology modeling

The homology models of CYP1A1 and CYP1B1 were generated by Modeller9.4[33] using the crystallographic structures of CYP1A2 (PDB ID: 2HI4)[34] and CYP2C9 (PDB ID: 1R9O)[35] as templates. The model of CYP1A1, residues Q32–S512, was based on sequence alignment with CYP1A2 (73% identity) as shown in Figure S1 (Supplementary data). The model of CYP1B1, residues R43–S525, was based on the multiple sequence alignment with both CYP1A2 (39% identity) and CYP2C9 (33% identity) shown in Figure S2 (Supplementary data). The lowest target function structure was selected among 30 models generated by Modeller and its quality was validated using the SAVS server.[36] The heme group was added after superimposing the homology models with the crystallographic structure of CYP1A2. Hydrogen atoms were added using the XLEaP module of Amber9,[37] which was used to apply the modified Amber force field ff99SB[38,39] to the protein atoms, and the parameters of Oda et al.[40] to the heme group. Subsequently, a set of minimization steps was carried out using the Sander module of Amber, so as to relax the models from crystal-packing contacts and optimize the position of the new atoms. In particular, 1000 steps were performed in order to allow relaxation of the hydrogen atoms only, using the steepest descent algorithm. Then, 1000 steps of conjugate gradient minimization were carried out by restraining only the Cα atoms with positional harmonic restraints of 50 kcal $mol^{-1}$ $Å^{-2}$ force constant. A third round of unrestrained minimization was carried out for 3000 steps. A distance-depended dielectric constant was employed throughout the energy minimizations with a 20-Å cutoff for the non-bonded interactions.

#### 4.5.2. Docking calculations

The 3D coordinates of the flavonoids were generated from their SMILES representation using Omega2.1.[41] AutoDockTools1.5.4 was employed for the preparation of proteins and ligands with the united-atom approximation.[42] All non-polar hydrogen atoms were merged, Gasteiger charges were assigned to the protein and ligand atoms, and the parameters of Oda et al.[40] were manually applied to the heme group. Docking calculations were performed using AutoDock4.2.[43] Grid maps were centered ~3 Å above the heme iron and comprised $81 \times 81 \times 81$ points of 0.375 Å spacing. For each complex, 100 docking calculations were performed using the Lamarckian genetic algorithm conformational search with default parameters from Autodock3.[44] The maximum number of energy evaluations was set to $25 \times 10^6$ and the resulted conformations were clustered within 2.0 Å root–mean–square positional deviation (rmsd). The most populated cluster with the highest affinity was selected after visual inspection of the docked conformations. In most cases, the top-ranked cluster exhibited the highest population, as in the case of the flavonoids shown in Figure 4. Detailed results from the docking calculation of CYP1A1 and CYP1B1 are given in Tables S1 and S2 (Supplementary data), respectively, in comparison with the experimental results. VMD 1.8.6 was used for analysis of the docking results and preparation of the figures.[45] All calculations were carried out on an x86_64 quad-core Intel workstation running linux2.6.29. AutoDock4.2 was compiled with gcc4.3 and Amber9 using Intel Fortran9.1.

## Supplementary data

Supplementary data associated with this article can be found, in the online version, at doi:10.1016/j.bmc.2011.03.042.

## References


1. Wang, J. F.; Zhang, C. C.; Chou, K. C.; Wei, D. Q. *Curr. Med. Chem.* **2009**, *16*, 232.
2. Pavek, P.; Dvorak, Z. *Curr. Drug Metab.* **2008**, *9*, 129.
3. Shimada, T.; Fujii-Kuriyama, Y. *Cancer Sci.* **2004**, *95*, 1.
4. Androutsopoulos, V. P.; Tsatsakis, A. M.; Spandidos, D. A. B. M. C. *Cancer* **2009**, *9*, 187.
5. Schwarz, D.; Roots, I. *Biochem. Biophys. Res. Commun.* **2003**, *303*, 902.
6. Schwarz, D.; Kisselev, P.; Roots, I. *Cancer Res.* **2003**, *63*, 8062.
7. Schwarz, D.; Kisselev, P.; Roots, I. *Eur. J. Cancer* **2005**, *41*, 151.
8. Ciolino, H. P.; Daschner, P. J.; Yeh, G. C. *Biochem. J.* **1999**, *340*, 715.
9. Ciolino, H. P.; Wang, T. T.; Yeh, G. C. *Cancer Res.* **1998**, *56*, 197.
10. Ciolino, H. P.; Yeh, G. C. *Br. J. Cancer* **1999**, *79*, 1340.
11. Birt, D. F.; Hendrich, S.; Wang, W. *Pharmacol. Ther.* **2001**, *90*, 157.
12. Wei, H. C.; Bowen, R.; Zhang, X. S.; Lebwohl, M. *Carcinogenesis* **1998**, *19*, 1509.
13. Doodstdar, H.; Burke, M. D.; Mayer, R. T. *Toxicology* **2000**, *144*, 31.
14. Takemura, H.; Uchiyama, H.; Ohura, T.; Sakakibara, H.; Kuruto, R.; Amagai, T.; Shimoi, K. *J. Steroid Biochem. Mol. Biol.* **2010**, *118*, 70.
15. Takemura, H.; Nagayoshi, H.; Matsuda, T.; Sakakibara, H.; Morita, M.; Matsui, A.; Ohura, T.; Shimoi, K. *Toxicology* **2010**, *274*, 42.
16. Androutsopoulos, V. P.; Papakyriakou, A.; Vourloumis, D.; Tsatsakis, A. M.; Spandidos, D. A. *Pharmacol. Ther.* **2010**, *126*, 9.
17. Androutsopoulos, V. P.; Arroo, R. R. J.; Hall, J. F.; Surichan, S.; Potter, G. A. *Breast Cancer Res.* **2008**, *10*, R39.
18. Androutsopoulos, V. P.; Wilsher, N.; Arroo, R. R. J.; Potter, G. A. *Cancer Lett.* **2009**, *274*, 54.
19. Androutsopoulos, V. P.; Mahale, S.; Arroo, R. R. J.; Potter, G. A. *Oncol. Rep.* **2009**, *21*, 1525.
20. Androutsopoulos, V. P.; Ruparelia, K.; Arroo, R. R. J.; Tsatsakis, A. M.; Spandidos, D. A. *Toxicology* **2009**, *264*, 162.
21. Zhai, S.; Dai, R.; Friedman, F. K.; Vestal, R. E. *Drug Metab. Dispos.* **1998**, *26*, 989.
22. Iori, F.; da Fonseca, R.; Ramos, M. J.; Menziani, M. C. *Bioorg. Med. Chem.* **2005**, *13*, 4366.
23. Takemura, H.; Itoh, T.; Yamamoto, K.; Sakakibara, H.; Shimoi, K. *Bioorg. Med. Chem.* **2010**, *18*, 6310.
24. Androutsopoulos, V. P.; Li, N.; Arroo, R. R. J. *J. Nat. Prod.* **2009**, *72*, 1390.
25. Yam, M. F.; Lim, V.; Salman, I. M.; Ameer, O. Z.; Ang, L. F.; Rosidah, N.; Abdulkarim, M. F.; Abdullah, G. Z.; Basir, R.; Sadikun, A.; Asmawi, M. Z. *Molecules* **2010**, *15*, 4452.
26. Itoh, T.; Takemura, H.; Shimoi, K.; Yamamoto, K. *J. Chem. Inf. Model.* **2010**, *50*, 1173.
27. Lewis, D. F.; Lake, B. G.; George, S. G.; Dickins, M.; Eddershaw, P. J.; Tarbit, M. H.; Beresford, A. P.; Goldfarb, P. S.; Guengerich, F. P. *Toxicology* **1999**, *139*, 53.
28. Lewis, D. F.; Lake, B. G.; Dickins, M. *Xenobiotica* **2004**, *34*, 501.
29. Lewis, D. F. V.; Gillam, E. M. J.; Everett, S. A.; Shimada, T. *Chem. Biol. Interact.* **2003**, *145*, 281.
30. Badawi, A. F.; Cavalieri, E. L.; Rogan, E. G. *Metabolism* **2001**, *50*, 1001.
31. Huang, Y. T.; Hwang, J. J.; Lee, P. P.; Ke, F. C.; Huang, J. H.; Huang, C. J.; Kandaswami, C.; Middleton, E.; Lee, M. T. *Br. J. Pharmacol.* **1999**, *128*, 999.
32. Ecay, T. W.; Dickson, J. L.; Conner, T. D. *Biochim. Biophys. Acta* **2000**, *1467*, 54.
33. Eswar, N.; John, B.; Mirkovic, N.; Fiser, A.; Ilyin, V. A.; Pieper, U.; Stuart, A. C.; Marti-Renom, M. A.; Madhusudhan, M. S.; Yerkovich, B.; Sali, A. *Nucleic Acids Res.* **2003**, *31*, 3375.
34. Sansen, S.; Yano, J. K.; Reynald, R. L.; Schoch, G. A.; Griffin, K. J.; Stout, C. D.; Johnson, E. F. *J. Biol. Chem.* **2007**, *282*, 14348.
35. Wester, M. R.; Yano, J. K.; Schoch, G. A.; Yang, C.; Griffin, K. J.; Stout, C. D.; Johnson, E. F. *J. Biol. Chem.* **2004**, *279*, 35630.
36. Stuctural Analysis and Verification Server. http://nihserver.mbi.ucla.edu/SAVS/ .
37. Case, D. A.; Cheatham, T. E., 3rd.; Darden, T.; Gohlke, H.; Luo, R.; Merz, K. M., Jr.; Onufriev, A.; Simmerling, C.; Wang, B.; Woods, R. J. *J. Comput. Chem.* **2005**, *26*, 1668.
38. Cornell, W. D.; Cieplak, P.; Bayly, C. I.; Gould, I. R.; Merz, K. M.; Ferguson, D. M.; Spellmeyer, D. C.; Fox, T.; Caldwell, J. W.; Kollman, P. A. *J. Am. Chem. Soc.* **1995**, *117*, 5179.
39. Hornak, V.; Abel, R.; Okur, A.; Strockbine, B.; Roitberg, A.; Simmerling, C. *Proteins* **2006**, *65*, 712.
40. Oda, A.; Yamaotsu, N.; Hirono, S. *J. Comput. Chem.* **2005**, *26*, 818.
41. Kirchmair, J.; Wolber, G.; Laggner, C.; Langer, T. *J. Chem. Inf. Model.* **2006**, *46*, 1848.
42. Sanner, M. F. *J. Mol. Graphics Modell.* **1999**, *17*, 57.
43. Huey, R.; Morris, G. M.; Olson, A. J.; Goodsell, D. S. *J. Comput. Chem.* **2007**, *28*, 1145.
44. Morris, G. M.; Goodsell, D. S.; Halliday, R. S.; Huey, R.; Hart, W. E.; Belew, R. K.; Olson, A. J. *J. Comput. Chem.* **1998**, *19*, 1639.
45. Humphrey, W.; Dalke, A.; Schulten, K. *J. Mol. Graph.* **1996**, *14*, 33.